

***Ab Initio* Electron-Phonon Interactions in Correlated Electron Systems**Jin-Jian Zhou^{1,2,*}, Jinsoo Park^{2,*}, Iurii Timrov³, Andrea Floris⁴, Matteo Cococcioni⁵,
Nicola Marzari³, and Marco Bernardi^{2,†}¹*School of Physics, Beijing Institute of Technology, Beijing 100081, China*²*Department of Applied Physics and Materials Science, California Institute of Technology,
Pasadena, California 91125, USA*³*Theory and Simulation of Materials (THEOS) and National Centre for Computational Design
and Discovery of Novel Materials (MARVEL), École Polytechnique Fédérale de Lausanne (EPFL),
CH-1015 Lausanne, Switzerland*⁴*School of Chemistry, University of Lincoln, Brayford Pool, Lincoln LN6 7TS, United Kingdom*⁵*Department of Physics, University of Pavia, Via A. Bassi 6, I-27100 Pavia, Italy*

(Received 19 February 2021; accepted 12 August 2021; published 16 September 2021)

Electron-phonon (e -ph) interactions are pervasive in condensed matter, governing phenomena such as transport, superconductivity, charge-density waves, polarons, and metal-insulator transitions. First-principles approaches enable accurate calculations of e -ph interactions in a wide range of solids. However, they remain an open challenge in correlated electron systems (CES), where density functional theory often fails to describe the ground state. Therefore reliable e -ph calculations remain out of reach for many transition metal oxides, high-temperature superconductors, Mott insulators, planetary materials, and multiferroics. Here we show first-principles calculations of e -ph interactions in CES, using the framework of Hubbard-corrected density functional theory (DFT + U) and its linear response extension (DFPT + U), which can describe the electronic structure and lattice dynamics of many CES. We showcase the accuracy of this approach for a prototypical Mott system, CoO, carrying out a detailed investigation of its e -ph interactions and electron spectral functions. While standard DFPT gives unphysically divergent and short-ranged e -ph interactions, DFPT + U is shown to remove the divergences and properly account for the long-range Fröhlich interaction, allowing us to model polaron effects in a Mott insulator. Our work establishes a broadly applicable and affordable approach for quantitative studies of e -ph interactions in CES, a novel theoretical tool to interpret experiments in this broad class of materials.

DOI: 10.1103/PhysRevLett.127.126404

Strongly correlated materials are at the center of exciting advances in condensed matter physics. These correlated electron systems (CES) can host states of matter ranging from high-temperature superconductivity [1] to Mott transitions [2,3], colossal magnetoresistance [4], and multiferroicity [5]. Electron-phonon (e -ph) interactions play an important role in these phenomena, often governing their origin and temperature dependence. A promising direction to study quantitatively e -ph interactions in CES is using first-principles calculations, where one employs density functional theory (DFT) to compute the electronic structure, density functional perturbation theory [6] (DFPT) for the lattice dynamics, and their combination to obtain the e -ph coupling [7,8]. This approach can successfully describe e -ph interactions and electron dynamics in a wide range of materials [7–20]. Recent work has extended this framework by combining the GW and DFPT approaches to reveal correlation-enhanced e -ph interactions in metallic systems [21,22].

However, computing e -ph interactions in CES remains challenging as standard DFT usually fails to describe their

ground state, mainly due to self-interaction errors in open subshells of localized d or f electrons. In addition, correlated transition metal oxides (TMOs) often exhibit strong e -ph coupling and polaron effects, requiring treatments beyond lowest-order perturbation theory [12]. Widely used first-principles approaches to compute the ground state of CES include DFT + U [23–26], hybrid functionals [27], and dynamical mean-field theory [28,29]. Developing accurate e -ph calculation in any of these frameworks is an important open challenge—if fulfilled, it would advance investigations of the rich physics of CES and significantly expand the scope of first-principles studies of e -ph interactions.

The DFT + U method [23–26] is particularly promising to mitigate the self-interaction error of DFT, using the Hubbard correction to better capture the physics of localized d electrons [30,31]. It can predict the ground state of various families of correlated TMOs, including Mott insulators [23], high-temperature superconductors [32], and multiferroics [33,34]. Its linear response variant, DFPT + U , has been employed successfully to study the

lattice dynamics of TMOs [35–38]. As the Hubbard- U value can be computed *ab initio* [39], as we do here, the framework is entirely free of empirical parameters.

In this Letter, we show calculations of e -ph interactions in the framework of DFT + U , focusing on a prototypical Mott insulator, cobalt oxide (CoO), as a case study. While DFT predicts CoO to be a dynamically unstable metal, DFT + U correctly predicts its antiferromagnetic insulating ground state [36,40]. We thus find that the long-range Fröhlich e -ph interaction is restored in DFPT + U , and unphysical divergences of the e -ph coupling due to spurious soft modes are removed. With the correct Fröhlich interaction in hand, we study the electron spectral function with a cumulant approach, revealing the formation of a polaron state with sharp quasiparticle and satellite peaks at low temperature that broaden and disappear entirely at room temperature. The Hubbard U -derived e -ph perturbation, missing in DFPT, is found to act primarily on the partially filled d bands of each spin channel, showing the impact of the d electron Coulomb repulsion on e -ph interactions. The DFT + U e -ph calculations developed in this work are poised to advance the understanding of e -ph coupling, transport, and superconductivity in strongly correlated materials.

For quantitative studies of e -ph interactions, of key interest are the e -ph matrix elements, $g_{m\nu}^{\sigma}(\mathbf{k}, \mathbf{q})$, which quantify the probability amplitude for an electron in a Bloch state $|\psi_{nk\sigma}\rangle$, with band index n , spin σ , and crystal momentum \mathbf{k} , to scatter into a final state $|\psi_{m\mathbf{k}+\mathbf{q}\sigma}\rangle$ by emitting or absorbing a phonon with mode index ν , wave-vector \mathbf{q} , energy $\hbar\omega_{\nu\mathbf{q}}$, and displacement eigenvector $\mathbf{e}_{\nu\mathbf{q}}$ [7,41,42],

$$g_{m\nu}^{\sigma}(\mathbf{k}, \mathbf{q}) = \left(\frac{\hbar}{2\omega_{\nu\mathbf{q}}}\right)^{\frac{1}{2}} \sum_I \frac{\mathbf{e}_{\nu\mathbf{q}}^I}{\sqrt{M_I}} \langle \psi_{m\mathbf{k}+\mathbf{q}\sigma} | d_{qI} \hat{V}^{\sigma} | \psi_{nk\sigma} \rangle, \quad (1)$$

where $d_{qI} \hat{V}^{\sigma} \equiv \sum_p e^{i\mathbf{q}\cdot\mathbf{R}_p} d_{pI} \hat{V}^{\sigma}$ is the e -ph perturbation due to the change of the potential acting on an electron with spin σ from a unit displacement of atom I (with mass M_I and located in the unit cell at \mathbf{R}_p).

In DFPT + U , besides the usual Kohn-Sham (KS) perturbation potential [41], there is an additional term from the perturbation of the Hubbard potential [36]:

$$d\hat{V}^{\sigma} = d\hat{V}_{\text{KS}}^{\sigma} + d\hat{V}_{\text{Hub}}^{\sigma}. \quad (2)$$

This Hubbard perturbation potential is the sum of projector and occupation-matrix derivative terms [36,43],

$$\begin{aligned} d\hat{V}_{\text{Hub}}^{\sigma} &= \sum_{I m_1 m_2} U^I \left(\frac{\delta_{m_1 m_2}}{2} - n_{m_1 m_2}^{I\sigma} \right) \partial \hat{P}_{m_1 m_2}^I \\ &\quad - \sum_{I m_1 m_2} U^I (d n_{m_1 m_2}^{I\sigma}) \hat{P}_{m_1 m_2}^I, \end{aligned} \quad (3)$$

where m_1 and m_2 are magnetic quantum numbers of the $3d$ orbitals, U^I is the effective Hubbard parameter for atom I ,

and $n_{m_1 m_2}^{I\sigma}$ is the occupation matrix for orbitals with magnetic quantum numbers m_1 and m_2 on atom I ,

$$n_{m_1 m_2}^{I\sigma} = \sum_{nk} \langle \psi_{nk\sigma} | \hat{P}_{m_2 m_1}^I | \psi_{nk\sigma} \rangle. \quad (4)$$

Here, \hat{P} is the generalized projector on the space of the localized atomic orbitals φ_m^I ,

$$\hat{P}_{m_2 m_1}^I = \hat{S} |\varphi_{m_2}^I\rangle \langle \varphi_{m_1}^I| \hat{S}, \quad (5)$$

and \hat{S} is the overlap operator of the ultrasoft pseudopotential [46]. In Eq. (3), the projector derivative term is efficiently computed with an analytical formula [36] while the occupation-matrix derivative $d n_{m_1 m_2}^{I\sigma}$ is computed with DFPT and includes contributions from the response of the wave functions to the atomic displacements [36]:

$$\begin{aligned} d n_{m_1 m_2}^{I\sigma} &= \sum_{nk} \langle \psi_{nk\sigma} | \partial \hat{P}_{m_2 m_1}^I | \psi_{nk\sigma} \rangle \\ &\quad + \sum_{nk} [\langle d\psi_{nk\sigma} | \hat{P}_{m_2 m_1}^I | \psi_{nk\sigma} \rangle \\ &\quad + \langle \psi_{nk\sigma} | \hat{P}_{m_2 m_1}^I | d\psi_{nk\sigma} \rangle]. \end{aligned} \quad (6)$$

We apply this framework to investigate the e -ph interactions and electron spectral functions in CoO, focusing on the effects of the Hubbard U correction [47]. The ground state electronic structure of CoO is obtained with collinear spin-polarized DFT + U calculations in a plane-wave basis using the QUANTUM ESPRESSO code [48]. We use the PBEsol exchange-correlation functional [49] and ultrasoft pseudopotentials [46] from the GBRV library [50]. We employ a 4-atom rhombohedral unit cell with relaxed lattice constants ($a = 5.206$ Å, $b = 3.019$ Å, $c = 3.009$ Å, and angle $\beta = 125.05^\circ$) and kinetic energy cutoffs of 60 Ry for the wave functions and 720 Ry for the charge density. Results for the 4-atom rhombohedral and 8-atom monoclinic unit cells [36] are nearly identical, as we have verified, so we choose the 4-atom unit cell for simplicity. Leveraging a recent implementation of DFPT + U [36,42], we compute the lattice dynamics and e -ph perturbation potentials on coarse irreducible \mathbf{q} -point grids. We then rotate the KS and Hubbard perturbation potentials with the PERTURBO code to obtain the e -ph matrix elements in the full Brillouin zone (BZ), using coarse grids with $8 \times 8 \times 8$ \mathbf{k} and \mathbf{q} points. The Wannier functions are obtained with the WANNIER90 code [51] and used in PERTURBO [41] to interpolate the e -ph matrix elements to finer grids. We use atomic orbitals as the basis for the Hubbard manifold. Our method is free of adjustable parameters, including the Hubbard U value, $U = 4.55$ eV for Co $3d$ states, which is determined *ab initio* with a linear response approach [36,39,52].

Using these quantities, we compute the lowest-order (Fan-Migdal) e -ph self-energy, $\Sigma_{nk\sigma}(\omega, T)$, at temperature

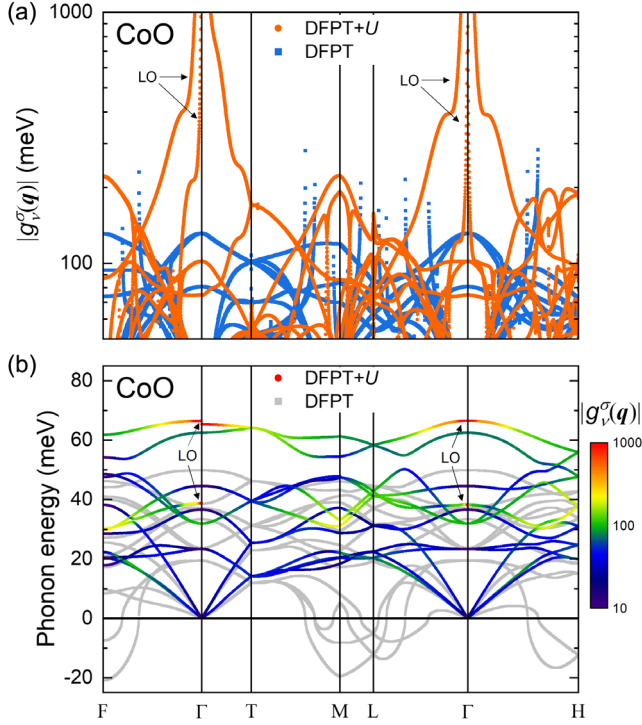


FIG. 1. (a) Comparison between the e -ph matrix elements in CoO computed with DFPT + U (orange) and standard DFPT (blue). Shown is $|g_\nu^\sigma(\mathbf{q})| \equiv (\sum_{mn} |g_{m\nu}^\sigma(\mathbf{k} = 0, \mathbf{q})|^2 / N_b)^{1/2}$ for all phonon modes ν , where the phonon wave vector \mathbf{q} is varied along high-symmetry BZ lines and the summation runs over the $N_b = 10$ spin-up Co $3d$ Wannier bands [56]. (b) CoO phonon dispersions overlaid with a log-scale color map of $|g_\nu^\sigma(\mathbf{q})|$ computed with DFPT + U (colored line). The CoO phonon dispersions from standard DFPT (gray line) are given for comparison, with imaginary frequencies shown as negative values.

T and electron energy ω , as implemented in PERTURBO [12,41]; the imaginary part is computed off-shell on a fine energy grid while the real part is evaluated on-shell at the band energy $\varepsilon_{nk\sigma}$. To capture strong e -ph interactions beyond the lowest-order, we use the finite-temperature cumulant approach described in Ref. [12]. The latter allows us to obtain the temperature-dependent retarded Green's function $G_{nk\sigma}^R(\omega)$ and the resulting electron spectral function, $A_{nk\sigma}(\omega) = -\text{Im}G_{nk\sigma}^R(\omega)/\pi$, which includes polaron effects such as band renormalization and satellite peaks [12,53–55]. Our framework therefore captures two key aspects of the physics of correlated TMOs, the effects of the localized Coulomb repulsion through DFT + U and the strong e -ph coupling and its temperature dependence with the finite-temperature cumulant approach.

The e -ph matrix elements from DFPT + U , which include effects from both the KS and Hubbard perturbations, are computed for the d bands of CoO in Fig. 1(a) and compared with results from standard DFPT [56]. The Hubbard U correction has a dramatic effect—the two sets of d band e -ph matrix elements differ widely, for all phonon

modes and everywhere in the BZ. The largest difference occurs near the zone center, where the DFPT + U results show the presence of the Fröhlich interaction [57], whereby the e -ph matrix elements diverge as $q \rightarrow 0$ for the longitudinal optical (LO) modes [10], whereas in plain DFPT they approach a finite value. The reason for this difference is subtle—although CoO is a semiconductor with a 2.5 eV band gap [58], DFT fails to properly describe its d electrons due to self-interaction errors and incorrectly predicts CoO to be a metal, so the Born effective charges and the Fröhlich interaction vanish in DFPT. When the Hubbard U correction is included, the self-interaction errors are mitigated and CoO is correctly predicted to be a polar semiconductor with divergent e -ph coupling for LO phonons near the zone center. This hallmark of the Fröhlich interaction is of critical importance for studies of transport and carrier dynamics in polar materials [10–12].

Figure 1(b) highlights the dramatic differences in the phonon dispersions computed with DFPT + U and plain DFPT [36]. In the latter, the ground state is dynamically unstable and the phonon dispersions exhibit soft phonon modes with imaginary frequencies. These errors are propagated to the e -ph interactions, resulting in e -ph matrix elements with unphysical divergences—near the F , M , L , and H points of the BZ in Fig. 1(a)—corresponding to zero-frequency phonon modes [see Eq. (1)] [11]. In DFPT + U , the ground state is stabilized to the correct antiferromagnetic phase, and the phonon dispersions are significantly improved [36] and in very good agreement with experiments [43]; the soft phonon modes are removed entirely and the e -ph matrix elements are well behaved throughout the BZ, without spurious divergences. These results underscore the importance of the Hubbard U correction for describing the electronic ground state and the resulting e -ph interactions in correlated TMOs.

In CoO, correcting the wave functions and charge density with DFT + U provides the main improvement to the e -ph coupling. To illustrate this point, Fig. 2 shows that the e -ph matrix elements computed with the KS perturbation alone but with DFT + U wave functions, $\tilde{g}_{\text{KS}} \propto \langle \psi_{\text{Hub}} | d\hat{V}_{\text{KS}} | \psi_{\text{Hub}} \rangle$, can capture both the Fröhlich interaction and the main trends in the e -ph coupling. Yet, the Hubbard perturbation potential $d\hat{V}_{\text{Hub}}$, which describes the effect of the lattice dynamics on the Hubbard U correction, also gives an important contribution. Figure 2 compares \tilde{g}_{KS} with the total DFPT + U e -ph matrix elements, $g_{\text{tot}} \propto \langle \psi_{\text{Hub}} | d\hat{V}_{\text{KS}} + d\hat{V}_{\text{Hub}} | \psi_{\text{Hub}} \rangle$, showing that both the KS and Hubbard terms are needed for quantitative accuracy. Direct DFPT + U calculations, shown in Fig. 2 as a benchmark, confirm this point and also validate our interpolation procedure.

Further analysis reveals that the contribution of the Hubbard e -ph perturbation is strongly band dependent and acts primarily on the partially filled $3d$ states of each spin channel [59]. To demonstrate this result, we compute

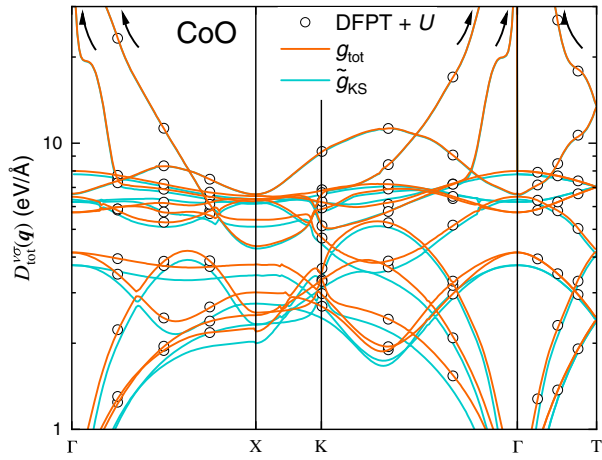


FIG. 2. Comparison between the e -ph coupling from the KS potential contribution alone (cyan line) and the total result including the Hubbard correction (orange line). In each case, we show the gauge-invariant e -ph coupling strength [41], $D_{\text{tot}}^{\nu\sigma}(\mathbf{q}) = (2\omega_{\nu\mathbf{q}} M_{\text{uc}} \sum_{nm} |g_{nm\nu}^{\sigma}(\mathbf{k} = 0, \mathbf{q})|^2 / N_b)^{1/2}$, computed, respectively, with e -ph matrix elements \tilde{g}_{KS} and g_{tot} , summing over all $N_b = 13$ highest spin-up valence bands. The BZ labeling refers to an equivalent (distorted) rocksalt structure [36]. Direct DFPT + U calculations (circles), shown as a benchmark, validate the Wannier interpolation. The arrows indicate the divergence due to the Fröhlich interaction.

the imaginary part of the e -ph self-energy [41] with contribution from only the Hubbard e -ph perturbation, and map it on the electronic spin-up band structure in Fig. 3(a). The plot shows the selective contribution of the Hubbard perturbation to e -ph processes in the partially filled $3d$ bands and the nearly negligible contribution in the completely filled $3d$ bands. The situation is analogous for the spin-down bands.

This trend is confirmed by studying the e -ph matrix elements in the Wannier basis, $g_{ij}(\mathbf{r}_p) \propto \langle \phi_i(0) | d\hat{V}(\mathbf{r}_p) | \phi_j(0) \rangle$ [41], computed using Co $3d$ Wannier functions ϕ_i and ϕ_j located on the same Co atom. These e -ph matrix elements decay exponentially with perturbation distance $|\mathbf{r}_p|$ due to the localized nature of the $3d$ Wannier functions. For these local e -ph interactions, we find that the KS and Hubbard contributions are nearly identical for the Co atom with partially filled spin-up $3d$ orbitals [Fig. 3(b)], whereas for the Co atom with completely filled spin-up $3d$ orbitals the Hubbard contribution is orders of magnitude smaller than the KS contribution [Fig. 3(c)] [59].

In TMOs, due to the polar bonds, electrons typically couple strongly with LO phonons via the Fröhlich interaction. In this common scenario, the e -ph interactions are strong enough to form large polarons, which can dominate transport and electron dynamical processes. The dominant coupling of electrons with LO phonons is clearly seen in Fig. 1(b), and thus we expect significant polaron effects in CoO. To investigate them, we compute the electron spectral

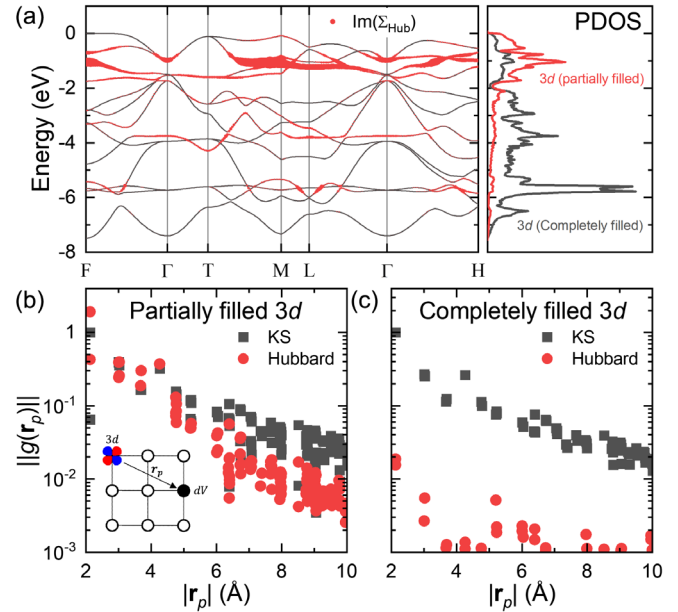


FIG. 3. (a) Band structure of CoO overlaid with the Hubbard contribution to the imaginary part of the e -ph self-energy, $\text{Im}(\Sigma_{\text{Hub}})$, for the representative case of the spin-up bands. The right panel shows the projected density of states (PDOS) of the partially and completely filled $3d$ orbitals. (b), (c) Comparison between the spatial decay of the real-space e -ph matrix elements for (b) the partially filled and (c) the completely filled $3d$ orbitals. Shown are the contributions from the KS (black squares) and Hubbard (red circles) e -ph perturbations [see Eq. (2)] to the maximum value of the Wannier basis matrix elements [8], $\|g(\mathbf{r}_p)\| = \max_{ij} |g_{ij}(\mathbf{r}_p)|$, normalized using the KS contribution. The inset in (b) is a schematic of the e -ph matrix elements in the Wannier basis, showing the atomic displacement perturbation at distance $|\mathbf{r}_p|$.

function with our recently developed finite-temperature cumulant approach, using the DFPT + U e -ph matrix elements as input [12].

Figure 4 shows the computed electron spectral functions at three temperatures between 100–300 K, for an electronic state near the top of the valence band. The spectral function at 100 K shows a sharp quasiparticle (QP) peak and two prominent sideband peaks, respectively, at energies ω_{LO} and $2\omega_{\text{LO}}$ below the QP peak, where $\omega_{\text{LO}} \approx 65$ meV is the energy of the zone center LO phonon with strongest e -ph coupling [see Fig. 1(b)]. These phonon sidebands are a hallmark of strong e -ph coupling and polaron effects [12]. Note that our calculations are performed with the Fermi energy lying above the valence band edge—a situation corresponding to lightly p -doped CoO—so the QP peak corresponds to a holelike QP excitation. Accordingly, the phonon sidebands appear at energy lower than the QP peak [60] and are associated with the simultaneous excitation of a holelike QP plus one or two LO phonons, respectively.

Because of a well-known sum rule, the spectral function integrates to one over energy, and thus the phonon

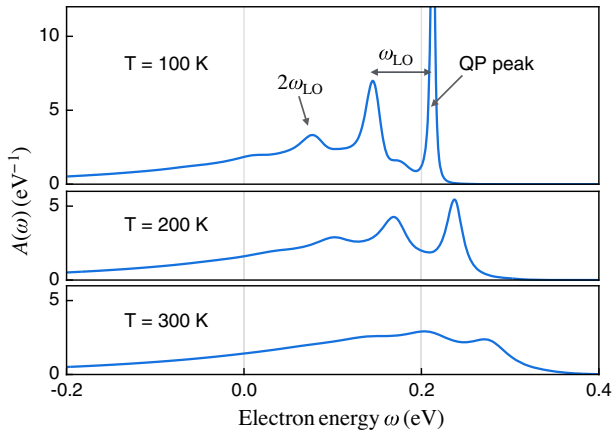


FIG. 4. Electron spectral function in CoO, computed at three temperatures from 100 to 300 K, for the highest valence band at crystal momentum $\mathbf{k} = \mathbf{F}$. In each panel, the zero of the electron energy ω is set to the band energy obtained from DFT + U calculations.

sidebands transfer spectral weight from the QP peak. In CoO, the QP spectral weight is strongly renormalized to a value of 0.2 at 100 K, with significant weight transfer to the phonon sidebands due to the strong e -ph interactions. As the temperature increases from 100 to 200 K, the QP peak becomes broader and overlaps with the phonon sidebands. At 300 K and higher temperatures, the peaks merge into a continuous background and the QP peak representing the original electronic state melts entirely into a polaron excitation. As the Fröhlich interaction making up the large polaron is entirely missing in DFT, our study of polaron effects in TMOs is enabled by the correct account of e -ph interactions in the DFT + U framework developed in this work.

In summary, we introduced an *ab initio* approach enabling quantitative calculations of e -ph interactions and polarons in correlated systems. Our method can be applied broadly to various families of strongly correlated materials with localized d or f electrons, leveraging the framework of parameter-free DFT + U . As shown in this work, our formalism can capture the strong coupling of electron, spin, and lattice degrees of freedom in CES and their combined effect on the e -ph interactions, paving the way for quantitative studies of the rich physics of various families of strongly correlated materials.

Work at Caltech was supported by the National Science Foundation under Grant No. DMR-1750613. J.-J. Z. was supported by the Joint Center for Artificial Photosynthesis, a DOE Energy Innovation Hub, supported through the Office of Science of the U.S. Department of Energy under Award No. DESC0004993. J. P. acknowledges support by the Korea Foundation for Advanced Studies. M. B. was partially supported by the Air Force Office of Scientific Research through the Young Investigator Program Grant

No. FA955018-1-0280. M. C., I. T., and N. M. acknowledge support from the EU-H2020 NFFA (Grant Agreement No. 654360). I. T. and N. M. also acknowledge support by the Swiss National Science Foundation (SNSF), through Grant No. 200021-179138, and its National Centre of Competence in Research (NCCR) MARVEL. A. F. thanks the UK's HEC Materials Chemistry Consortium, funded by EPSRC (EP/L000202, EP/R029431). This research used resources of the National Energy Research Scientific Computing Center (NERSC), a U.S. Department of Energy Office of Science User Facility located at Lawrence Berkeley National Laboratory, operated under Contract No. DE-AC02-05CH11231.

*These authors contributed equally to this work.

†Corresponding author.

bmarco@caltech.edu

- [1] W. E. Pickett, *Rev. Mod. Phys.* **61**, 433 (1989).
- [2] N. F. Mott, *Proc. Phys. Soc. London Sect. A* **62**, 416 (1949).
- [3] N. F. Mott, *Rev. Mod. Phys.* **40**, 677 (1968).
- [4] A. P. Ramirez, *J. Phys.* **9**, 8171 (1997).
- [5] H. Schmid, *Ferroelectrics* **162**, 317 (1994).
- [6] S. Baroni, S. de Gironcoli, A. Dal Corso, and P. Giannozzi, *Rev. Mod. Phys.* **73**, 515 (2001).
- [7] M. Bernardi, *Eur. Phys. J. B* **89**, 239 (2016).
- [8] L. A. Agapito and M. Bernardi, *Phys. Rev. B* **97**, 235146 (2018).
- [9] M. Bernardi, D. Vigil-Fowler, J. Lischner, J. B. Neaton, and S. G. Louie, *Phys. Rev. Lett.* **112**, 257402 (2014).
- [10] J.-J. Zhou and M. Bernardi, *Phys. Rev. B* **94**, 201201(R) (2016).
- [11] J.-J. Zhou, O. Hellman, and M. Bernardi, *Phys. Rev. Lett.* **121**, 226603 (2018).
- [12] J.-J. Zhou and M. Bernardi, *Phys. Rev. Research* **1**, 033138 (2019).
- [13] C.-H. Park, F. Giustino, M. L. Cohen, and S. G. Louie, *Phys. Rev. Lett.* **99**, 086804 (2007).
- [14] A. Floris, A. Sanna, S. Massidda, and E. K. U. Gross, *Phys. Rev. B* **75**, 054508 (2007).
- [15] J. Sjakste, I. Timrov, P. Gava, N. Mingo, and N. Vast, *Annual review of heat transfer* **17**, 333 (2014).
- [16] W. Li, *Phys. Rev. B* **92**, 075405 (2015).
- [17] T.-H. Liu, J. Zhou, B. Liao, D. J. Singh, and G. Chen, *Phys. Rev. B* **95**, 075206 (2017).
- [18] J. Ma, A. S. Nissimagoudar, and W. Li, *Phys. Rev. B* **97**, 045201 (2018).
- [19] S. Poncé, E. R. Margine, and F. Giustino, *Phys. Rev. B* **97**, 121201(R) (2018).
- [20] J. Park, J.-J. Zhou, and M. Bernardi, *Phys. Rev. B* **101**, 045202 (2020).
- [21] Z. Li, G. Antonius, M. Wu, F. H. da Jornada, and S. G. Louie, *Phys. Rev. Lett.* **122**, 186402 (2019).
- [22] Z. Li, M. Wu, Y.-H. Chan, and S. G. Louie, *Phys. Rev. Lett.* **126**, 146401 (2021).
- [23] V. I. Anisimov, J. Zaanen, and O. K. Andersen, *Phys. Rev. B* **44**, 943 (1991).
- [24] V. I. Anisimov, I. S. Elfimov, N. Hamada, and K. Terakura, *Phys. Rev. B* **54**, 4387 (1996).

- [25] V. I. Anisimov, F. Aryasetiawan, and A. I. Lichtenstein, *J. Phys.* **9**, 767 (1997).
- [26] S. L. Dudarev, G. A. Botton, S. Y. Savrasov, C. J. Humphreys, and A. P. Sutton, *Phys. Rev. B* **57**, 1505 (1998).
- [27] J. Heyd, G. E. Scuseria, and M. Ernzerhof, *J. Chem. Phys.* **118**, 8207 (2003).
- [28] A. Georges, G. Kotliar, W. Krauth, and M. J. Rozenberg, *Rev. Mod. Phys.* **68**, 13 (1996).
- [29] G. Kotliar, S. Y. Savrasov, K. Haule, V. S. Oudovenko, O. Parcollet, and C. A. Marianetti, *Rev. Mod. Phys.* **78**, 865 (2006).
- [30] H. J. Kulik, M. Cococcioni, D. A. Scherlis, and N. Marzari, *Phys. Rev. Lett.* **97**, 103001 (2006).
- [31] H. J. Kulik, *J. Chem. Phys.* **142**, 240901 (2015).
- [32] S. Pesant and M. Côté, *Phys. Rev. B* **84**, 085104 (2011).
- [33] P. Baettig, C. Ederer, and N. A. Spaldin, *Phys. Rev. B* **72**, 214105 (2005).
- [34] J. M. Rondinelli, A. S. Eidelson, and N. A. Spaldin, *Phys. Rev. B* **79**, 205119 (2009).
- [35] A. Floris, S. de Gironcoli, E. K. U. Gross, and M. Cococcioni, *Phys. Rev. B* **84**, 161102(R) (2011).
- [36] A. Floris, I. Timrov, B. Himmetoglu, N. Marzari, S. de Gironcoli, and M. Cococcioni, *Phys. Rev. B* **101**, 064305 (2020).
- [37] M. Blanchard, E. Balan, P. Giura, K. Béneut, H. Yi, G. Morin, C. Pinilla, M. Lazzeri, and A. Floris, *Phys. Chem. Miner.* **41**, 289 (2014).
- [38] K. Miwa, *Phys. Rev. B* **97**, 075143 (2018).
- [39] I. Timrov, N. Marzari, and M. Cococcioni, *Phys. Rev. B* **98**, 085127 (2018).
- [40] U. D. Wdowik and K. Parlinski, *Phys. Rev. B* **75**, 104306 (2007); **78**, 224114 (2008).
- [41] J.-J. Zhou, J. Park, I.-T. Lu, I. Maliyov, X. Tong, and M. Bernardi, *Comput. Phys. Commun.* **264**, 107970 (2021).
- [42] P. Giannozzi *et al.*, *J. Phys. Condens. Matter* **29**, 465901 (2017).
- [43] See Supplemental Material at <http://link.aps.org/supplemental/10.1103/PhysRevLett.127.126404> for additional derivations on the projector derivatives, and comparison of the computed phonon dispersion in CoO with experimental data, which includes Refs. [44,45].
- [44] J. Sakurai, W. J. L. Buyers, R. A. Cowley, and G. Dolling, *Phys. Rev.* **167**, 510 (1968).
- [45] M. H. Nassir and M. A. Langell, *Solid State Commun.* **92**, 791 (1994).
- [46] D. Vanderbilt, *Phys. Rev. B* **41**, 7892 (1990).
- [47] The data used to produce the results of this work are available on the Materials Cloud Archive, as follows: J.-J. Zhou, J. Park, I. Timrov, A. Floris, M. Cococcioni, N. Marzari, and M. Bernardi, Materials Cloud Archive 2021.141 (2021), <https://doi.org/10.24435/materialscloud:jt-32>.
- [48] P. Giannozzi *et al.*, *J. Phys. Condens. Matter* **21**, 395502 (2009).
- [49] J. P. Perdew, A. Ruzsinszky, G. I. Csonka, O. A. Vydrov, G. E. Scuseria, L. A. Constantin, X. Zhou, and K. Burke, *Phys. Rev. Lett.* **100**, 136406 (2008).
- [50] K. F. Garrity, J. W. Bennett, K. M. Rabe, and D. Vanderbilt, *Comput. Mater. Sci.* **81**, 446 (2014).
- [51] G. Pizzi *et al.*, *J. Phys.: Condens. Matter* **32**, 165902 (2020).
- [52] I. Timrov, N. Marzari, and M. Cococcioni, *Phys. Rev. B* **103**, 045141 (2021).
- [53] F. Aryasetiawan, L. Hedin, and K. Karlsson, *Phys. Rev. Lett.* **77**, 2268 (1996).
- [54] S. M. Story, J. J. Kas, F. D. Vila, M. J. Verstraete, and J. J. Rehr, *Phys. Rev. B* **90**, 195135 (2014).
- [55] J. P. Nery, P. B. Allen, G. Antonius, L. Reining, A. Miglio, and X. Gonze, *Phys. Rev. B* **97**, 115145 (2018).
- [56] As the Hubbard U correction reorders the band energies, to make a meaningful comparison in Fig. 1(a) we average the e -ph coupling over the entire set of 10 $3d$ bands, for both the DFPT and DFPT + U calculations.
- [57] H. Fröhlich, *Adv. Phys.* **3**, 325 (1954).
- [58] J. van Elp, J. L. Wieland, H. Eskes, P. Kuiper, G. A. Sawatzky, F. M. F. de Groot, and T. S. Turner, *Phys. Rev. B* **44**, 6090 (1991).
- [59] Note that there are two Co atoms in the unit cell of CoO, each generating a set of $3d$ bands in the solid; for each spin channel, due to the antiferromagnetic ground state of CoO, one set of $3d$ bands is completely filled and the other is partially filled.
- [60] A. Damascelli, Z. Hussain, and Z.-X. Shen, *Rev. Mod. Phys.* **75**, 473 (2003).